search at Stanford University. Support for the work done at Stanford Synchrotron Radiation Laboratory, which is operated by the Department of Energy, Division of Chemical Sciences, is gratefully acknowledged. P.M.J. would also like to acknowledge the IBM Corp. for its financial support.

Registry No. ZnO, 1314-13-2; CuCl, 7758-89-6; NH_3, 7664-41-7.

Supplementary Material Available: Tables giving the ground-state energies and valence level charge decomposition (%) for $[ZnO_3]^{4-}$ and $[CuCl_3]^{2-}$ (2 pages). Ordering information is given on any current masthead page.

Contribution from the Département de chimie, Université de Sherbrooke, Sherbrooke, Québec, Canada J1K 2R1, and Contribution No. 8446 from the Arthur Amos Noyes Laboratory, California Institute of Technology, Pasadena, California 91125

Silver and Gold Dimers. Crystal and Molecular Structures of $Ag_2(dmpm)_2Br_2$ and $[Au_2(dmpm)_2](PF_6)_2$ and Relation between Metal–Metal Force Constants and Metal–Metal Separations

Daniel Perreault,[1a] Marc Drouin,[1a] André Michel,*[,1a,c] Vincent M. Miskowski,[1b] William P. Schaefer,*[,1b,c] and Pierre D. Harvey*[,1a]

Received June 21, 1991

The $Ag_2(dmpm)_2Br_2$ and $[Au_2(dmpm)_2](PF_6)_2$ compounds (dmpm = bis(dimethylphosphino)methane) have been characterized by X-ray diffraction at 298 K. The molecules are found to contain $M_2(dmpm)_2^{2+}$ core structures with two metal atoms bridged by the dmpm ligands to give eight-membered $M_2P_4C_2$ rings. The silver compound forms a polymeric chain where the silver atoms of adjacent $Ag_2(dmpm)_2^{2+}$ units are linked by two Br anions (r(AgBr) = 2.7431 (13), 2.9453 (14) Å). The intra- and intermolecular Ag···Ag separations are 3.605 (2) and 3.916 (2) Å, respectively, while the Au···Au distance in $[Au_2(dmpm)_2](PF_6)_2$ is 3.045 (1) Å. In the latter case, some weak Au···F contacts (r(AuF) = 3.44 (1) Å) are also noticed. The solid-state low-frequency (40–400 cm^{-1}) vibrational spectra of these compounds and five other related complexes containing Ag_2 and Au_2 have been analyzed. Intense Raman scatterings associated with the metal–metal stretching frequencies ($\nu(M_2)$) along with the metal–metal force contants ($F(M_2)$; estimated from the diatomic approximation) have been obtained. The $\nu(M_2)$ (cm^{-1}) and $F(M_2)$ (mdyn $Å^{-1}$) values are as follows, respectively: $[Ag_2(dmpm)_2](PF_6)_2$, 76 and 0.18; $[Ag_2(dppm)_3](PF_6)_2$ (dppm = bis(diphenylphosphino)methane), 76 and 0.18; $[Au_2(dmpm)_2](PF_6)_2$, 68 and 0.27; $[Au_2(dmpm)_3](PF_6)_2$, 69 and 0.28; $[Au_2(dmpm)_2]Cl_2$, 71 and 0.29; $Au_2(dmb)(CN)_2$ (dmb = 1,8-diisocyano-*p*-menthane), 36 and 0.075. Including literature results, data banks of four and eleven points are accumulated for the silver and gold compounds, respectively, where reparametrized Herschbach–Laurie type relationships (H–L) between $r(M_2)$ and $F(M_2)$ applied to Ag_2 or Au_2 systems are designed. For $Ag_2(dmpm)_2Br_2$ ($\nu(Ag_2)$ = 48 cm^{-1}), the estimated $F(Ag_2)$ for the intramolecular Ag···Ag interactions is 0.03 mdyn $Å^{-1}$. Crystallographic details are as follows. For $Ag_2(dmpm)_2Br_2$: monoclinic space group $P2_1/n$, a = 7.2023 (8) Å, b = 10.5734 (5) Å, c = 14.1980 (6) Å, β = 82.466 (9)°, Z = 2, R = 0.040 for 1382 reflections measured. For $[Au_2(dmpm)_2](PF_6)_2$: monoclinic space group $C2/m$, a = 10.234 (1) Å, b = 13.711 (2) Å, c = 9.525 (2) Å, β = 96.74 (1)°, Z = 2, R = 0.050 for 1540 reflections where $F_o^2 > 3\sigma(F_o^2)$.

Introduction

Empirical equations relating atom–atom distances (r) and atom–atom force constants (F),[2,3] or atom–atom stretching frequencies (ν),[4,5] are numerous. The reported equations relating r and F have different mathematical forms going from Badger's ($r = a + b(F^{-1/3})$)[2a] to Herschbach and Laurie's ($r = a + b(\log F)$)[2b] to Woodruff's rules ($r = a + b\exp(-F/c)$).[3] The latest ones have been specifically designed to include systems containing M_2 units for which the M_2 separations were relatively long and have been succesfully used for M_2 complexes (M = Rh, Pd, Pt).[6] In the family of diphosphine M_2 complexes exhibiting long $r(M_2)$ are found the Ag_2 and Au_2 compounds.[7,8] We are interested in these systems, since they exhibit long-lived lowest energy excited states (0.2–2.4 μs) and their photochemical reactivity and photophysical properties depend, in part, upon the M_2 interactions.[8j,9]

Recently we have reported the preparation and characterization of the luminescent compound $Au_2(tmb)Cl_2$ (tmb = 2,5-dimethyl-2′,5′-diisocyanohexane), in which no intramolecular Au_2 interactions occur; however, small intermolecular Au···Au contacts ($r(Au_2)$ = 3.3 Å) are observed in the solid state.[10] Indeed, an intense $\nu(Au_2)$ Raman band located at 50 cm^{-1} was assigned, and an associated $F(Au_2)$ of 0.14 mdyn $Å^{-1}$ was reported for these interactions. Also, Che et al.[8j] have published the crystal structure of $Au_2(dmb)(CN)_2$ (dmb = 1,8-diisocyano-*p*-menthane), for which, while the intramolecular Au_2 interaction ($r(Au_2)$ = 3.536 (1) Å) is weak, clear molecular distortions favoring the Au_2 interactions are nonetheless observed. M_2 systems exhibiting very weak M_2 interactions are not uncommon. For instance, $Hg_2(^1\Sigma_g^+)$ and $Hg_2(^1\Sigma_u^+)$ also exhibit long $r(Hg_2)$ and low $\nu(Hg_2)$ ($r(Hg_2)$ = 3.63 ● 0.04 and 3.61 ± 0.05 Å and $\nu(Hg_2)$ = 18.5 ● 0.5 and

* To whom correspondence should be addressed.

(1) (a) Université de Sherbrooke. (b) California Institute of Technology. (c) All correspondance pertaining the crystallography studies should be addressed to these authors.
(2) (a) Badger, R. M. *J. Chem. Phys.* **1934**, *2*, 128; **1935**, *3*, 710. (b) Hershbach, D. R.; Laurie, V. W. *J. Chem. Phys.* **1961**, *35*, 458.
(3) (a) Miskowski, V. M.; Dallinger, R. F.; Christoph, G. G.; Morris, D. E.; Spies, G. H.; Woodruff, W. H. *Inorg. Chem.* **1987**, *26*, 2127. (b) Conradson, S. D.; Sattelberger, A. P.; Woodruff, W. H. *J. Am. Chem. Soc.* **1988**, *110*, 1309. (c) Woodruff, W. H. Unpublished results.
(4) (a) Butler, I. S.; Harvey, P. D.; McCall, J. M.; Shaver, A. *J. Raman Spectrosc.* **1986**, *17*, 221. (b) Steudel, R. *Z. Naturforsch.* **1975**, *30B*, 281.
(5) Codier, C. Ph.D. Thesis, Université Paris VI, 1991.
(6) (a) Harvey, P. D.; Gray, H. B. *J. Am. Chem. Soc.* **1988**, *110*, 4391. (b) Harvey, P. D.; Adar, F.; Gray, H. B. *J. Am. Chem. Soc.* **1989**, *111*, 1312.
(7) (a) Ho, D. M.; Bau, R. *Inorg. Chem.* **1983**, *22*, 4073. (b) Tiekink, E. R. T. *Acta Crystallogr.* **1990**, *C46*, 235. (c) Karsh, H. H.; Schubert, U. *Z. Naturforsch.* **1982**, *B37*, 186.
(8) (a) Schmidbaur, H.; Pollok, Th.; Herr, R.; Wagner, F. E.; Bau, R.; Riede, J.; Müller, G. *Organometallics* **1986**, *5*, 566. (b) Schmidbaur, H.; Wohlleben, A.; Schubert, U.; Frank, A.; Huttner, G. *Chem. Ber.* **1977**, *110*, 2751. (c) Schmidbaur, H.; Mandl, J. R.; Bassett, J.-M.; Blaschke, G.; Zimmer-Gasser, B. *Chem. Ber.* **1981**, *114*, 433. (d) Briant, C. E.; Hall, K. P.; Mingos, D. M. P. *J. Organomet. Chem.* **1982**, *229*, C5. (e) Kozelka, J.; Oswald, H. R.; Dubler, E. *Acta Crystallogr.* **1986**, *C42*, 1007. (f) Bensch, W.; Prelati, M.; Ludwig, W. *J. Chem. Soc., Chem. Commun.* **1986**, 1762. (g) Payne, N. C.; Puddephatt, R. J.; Ravindranath, R.; Treunicht, I. *Can. J. Chem.* **1988**, *66*, 3176. (h) Jaw, H.-R. C.; Savas, M. M.; Rodgers, R. D.; Mason, W. R. *Inorg. Chem.* **1989**, *28*, 1028. (i) Khan, Md. N. I.; King, C.; Heinrich, D. D.; Fackler, J. P., Jr.; Porter, L. C. *Inorg. Chem.* **1989**, *28*, 2150. (j) Che, C.-M.; Wong, W.-T.; Lai, T.-F.; Kwong, H.-L. *J. Chem. Soc., Chem. Commun.* **1989**, 243.

0020-1669/92/1331-0695$03.00/0

19.7 ± 0.5 cm^{-1}, respectively).[11]

Woodruff's rules for the 4d and 5d elements are[3]

$$r(4d) = 1.82 + 1.46 \exp(-F/2.61) \quad (1)$$

$$r(5d) = 2.04 + 1.32 \exp(-F/2.17) \quad (2)$$

For F values approaching zero, r(4d) and r(5d) reach their limiting values of 3.28 and 3.36 Å, respectively. Mathematically, these equations are inadequate for $r(M_2) > 3.36$ Å. We have also noticed that Woodruff's rules apply with some difficulty for the Ag_2 and Au_2 compounds with respect to the Pd_2 and Pt_2 complexes. In this work, we wish to report the single-crystal X-ray diffraction structures of two M_2 dmpm complexes, $Ag_2(dmpm)_2Br_2$ and $[Au_2(dmpm)_2](PF_6)_2$ (dmpm = bis(dimethylphosphino)methane), and low-frequency solid-state Raman and IR spectra for these compounds as well as for related diphosphine and diisocyanide Ag_2 and Au_2 complexes for which the $r(M_2)$ values are known. Using literature results ($r(M_2)$ and $\nu(M_2)$) on other M_2 compounds, reparametrized Herschbach–Laurie type relationships (H–L) for silver and gold polynuclear complexes are designed.

Experimental Section

Materials. $[Ag_2(dmpm)_2](PF_6)_2$,[7c] $[Ag_2(dppm)_3](PF_6)_2$,[12,13] $Au_2(dmb)(CN)_2$,[11] $Pd_2(dppm)_3$,[14] $Pt_2(dppm)_3$,[15] and $Pd_2(dmb)_2(CN)_4$[16] were prepared according to standard procedures. dmpm and dppm were purchased from Strem Chemical Co. and were used without purification.

Ag_2(dmpm)$_2Br_2$. A 1.0-mmol sample of AgBr was suspended in a 1.3 mmol of dmpm in benzene (10 mL) solution under Ar(g) atmosphere. After 2 h of stirring, the white solid deposited slowly and was immediately filtered off in air, washed with a minimum of water and a minimum amount of ethanol, and then recrystallized by slow evaporation of an acetonitrile solution. The recrystallization produced large crystals (chemical yield based on silver bromide is ~80%) which were suitable for X-ray crystallographic studies. The product was then identified by single-crystal X-ray diffraction. IR: 2965 w, 2897 w (ν(C–H)), 2855 w, 1418 m, 1360 m, 1277 m, 936 s, 909 s. $^{31}P\{^1H\}$ NMR (CD_2Cl_2; 298 K): δ_P = 29.4 ppm vs external standard 85% H_3PO_4, fwhm = 250 Hz.

$[Au_2$(dmpm)$_2](PF_6)_2$. Method 1. $[Au_2(dmpm)_2](PF_6)_2$ was prepared according to the procedure outlined for $[Au_2(dmpm)_2](ClO_4)_2$,[8h] except that HPF_6 (Aldrich) was used instead of $HClO_4$. Yield: 33%. The white powder was recrystallized from acetonitrile solutions. Anal. Calcd for $Au_2C_{10}H_{28}F_{12}P_6$: C, 12.56; H, 2.95. Found: C, 12.40; H, 2.80. $^{31}P\{^1H\}$ NMR (CD_3CN; 298 K): δ_P = 15.9 ppm vs external standard 85% H_3PO_4. The crystals are air stable.

Method 2. To a 50-mL benzene solution of 1.17 mmol of Et_3PAuCl (Strem) under N_2 atmosphere was added an equimolar amount of dmpm, precipitating $[Au_2(dmpm)_2]Cl_2$. The latter was dissolved in 10 mL of methanol. Dropwise addition of a concentrated solution of $NaPF_6$ in methanol produced a white precipitate of $[Au_2(dmpm)_2](PF_6)_2$. The compound was recrystallized from acetonitrile/ether by vapor diffusion, providing crystals of suitable quality for X-ray crystallographic analysis. Yield: >70%. Anal. Calcd (found): C, 12.56 (12.59); H, 2.95 (2.87).

$[Au_2$(dmpm)$_3](PF_6)_2$. To a $[Au_2(dmpm)_2](PF_6)_2$ acetonitrile solution (0.51 mmol in 20 mL) under N_2 was added a 3-fold excess of dmpm. Addition of a minimum amount of ether yielded a pale yellow powder in quantitative yield. The compound was recrystallized from acetonitrile/ether by vapor diffusion. Anal. Calcd (found): C, 16.50 (16.53); H, 3.88 (3.70). $^{31}P\{^1H\}$ NMR (CD_3CN; 298 K): δ_P = 16.9 ppm vs external standard 85% H_3PO_4.

Instruments. The Raman spectra were measured on an Instruments SA Raman spectrometer equipped with a U-1000 Jobin-Yvon 1.0-m double monochromator using the 647.1-nm red line and the 514.5-nm green line of Spectra-Physics krypton and argon ion lasers, respectively, for excitation. The far-IR spectra were measured on a FT-BOMEM DA 3.002 spectrometer with a resolution of 4 cm^{-1}, typically using from 50 to 256 scans.

Crystallographic Data. Ag_2(dmpm)$_2Br_2$. A clear cubic single crystal was mounted on an Enraf-Nonius CAD-4 diffractometer, using a graphite monochromator and Mo Kα radiation (λ = 0.71073 Å) with an $\omega/2\theta$ scan at a constant speed of 2.7° min^{-1}. Clear crystal: 0.30 × 0.35 × 0.30 mm, M_r = 647.76, monoclinic, a = 7.2023 (8) Å, b = 10.5734 (5) Å, c = 14.1980 (6) Å, β = 82.466 (9)°, V = 1071.9(1) $Å^3$, space group $P2_1/n$, Z = 2, D_{calcd} = 2.007 g cm^{-3}, μ(Mo Kα) = 57.90 cm^{-1}. The lattice parameters were refined from 24 reflections with a 2θ range of 35–45° (index limits: $h = \pm 7$; $k = +10$; $l = +15$) remeasuring 2 standard reflections every 60 min. A total of 1382 unique measured reflections were collected, of which 1061 we considered observed ($I_{net} \geq 2.5\sigma(I_{net})$). An analytical linear absorption correction was applied with minimum and maximum transmission factors of 0.195037 and 0.212958. All non-H atoms were refined anisotropically. The hydrogen positions were all calculated but not refined. The final residuals at convergence were R = 0.040, R_w = 0.027, and S = 3.048; $(\Delta/\sigma)_{max}$ = 0.032, and the secondary extinction coefficient was 0.207 (8).[17a] The maximum and minimum density peaks in the final difference Fourier map were 0.56 and −0.76 e $Å^{-3}$. The structure was solved by direct methods and refined using the NRCVAX system.[17b] Weights based on counting statistics were used. The function $\sum w(|F_o| - |F_c|)^2$ with $w = 1/(\sigma^2(F_o))$ was minimized. Scattering factors were taken from ref 17c. Crystal data and collection parameters are listed in Table I.

$[Au_2$(dmpm)$_2](PF_6)_2$. A translucent crystal was obtained: 0.23 × 0.38 × 0.35 mm, monoclinic system, space group $C2/m$ (No. 12), with a = 10.234 (1) Å, b = 13.711 (2) Å, c = 9.525 (2) Å, β = 96.74 (1)°, V = 1327.3 (4) $Å^3$; Z = 2, and density = 2.39 g cm^{-3}. The single crystal chosen was glued with epoxy cement to a glass fiber. The crystal was centered on the diffractometer, and unit cell dimensions and an orientation matrix were obtained from the setting angles of 25 reflections with $15° < 2\theta < 20°$. A shell of data to $2\theta \leq 50°$ was collected, and new cell dimensions were calculated from the setting angles of 25 different reflections with $36° < 2\theta < 45°$. A shell of data with $50° < 2\theta < 60°$ completed the data set. There were no absences in the data other than those due to the centered cell, indicating space group $C2$, Cm, or $C2/m$.

Table I. Crystallographic Data for $Ag_2(dmpm)_2Br_2$ and $[Au_2(dmpm)_2](PF_6)_2$

formula	$Ag_2Br_2C_{10}H_{28}P_4$	$Au_2C_{10}H_{28}P_6F_{12}$
fw	647.76	956.09
space gp	$P2_1/n$	$C2/m$
a/Å	7.2023 (8)	10.234 (1)
b/Å	10.5734 (5)	13.711 (2)
c/Å	14.1980 (6)	9.525 (2)
β/deg	82.466 (9)	96.74 (1)
V/$Å^3$	1071.9 (1)	1327.3 (4)
Z	2	2
T/°C	20	23
λ/Å	0.71073	0.71073
D_{calcd}/g cm^{-3}	2.007	2.39
μ/cm^{-1}	57.9	118.26
transm coeff	0.195–0.213	0.051–0.140
R	0.040	0.050
R_w	0.030	0.015 (on F^2)

(9) (a) King, C.; Wang, J.-C.; Khan, Md. N. I.; Fackler, J. P., Jr. *Inorg. Chem.* **1989**, *28*, 2145. (b) Caspar, J. V. *J. Am. Chem. Soc.* **1985**, *107*, 6718. (c) Harvey, P. D.; Dallinger, R. F.; Woodruff, W. H.; Gray, H. B. *Inorg. Chem.* **1989**, *28*, 3057.

(10) Perreault, D.; Drouin, M.; Michel, A.; Harvey, P. D. *Inorg. Chem.* **1991**, *30*, 2.

(11) Van Zee, R. D.; Blankespoor, S. C.; Zwier, T. S. *J. Chem. Phys.* **1988**, *88*, 4650.

(12) $[Ag_2(dppm)_3](PF_6)_2$ was synthesized according to the procedure outlined for $[Ag_2(dppm)_3](CF_3SO_3)_2$[13] except that $AgPF_6$ was used instead of $AgCF_3SO_3$. Anal. Calcd for $P_8C_{15}H_{42}F_{12}Ag_2$: C, 18.70; H, 4.36; P, 25.72; F 22.38. Found: C, 19.02; H, 4.30; P, 25.65; F, 28.65. ^{31}P NMR (CD_2Cl_2; 298 K): δ_P 10.3 ppm vs external standard 85% H_3PO_4.

(13) Obendorf, D.; Probet, M.; Peringer, P.; Falk, H.; Muller, N. *J. Chem. Soc., Dalton Trans.* **1988**, 1709.

(14) Stern, E. W.; Maples, P. K. *J. Catal.* **1972**, *27*, 120.

(15) Grossel, M. C.; Brown, M. P.; Nelson, C. D.; Yavari, A.; Kallas, E.; Moulding, R. P.; Seddon, D. R. *J. Organomet. Chem.* **1982**, *232*, C13.

(16) (a) $Pd_2(dmb)_2(CN)_4$ was synthesized according to the procedure given for $Pt_2(dppm)_2(CN)_4$[16b] except $Pd(CN)_2 \cdot nH_2O$ (Strem) and dmb were used instead of $Pt(CN)_2$ and dppm, respectively. Anal. Calcd for $C_{28}H_{36}N_8Pd_2$: C, 48.22; H, 5.20; N, 16.07. Found: C, 48.31; H, 5.42; N, 15.82. Details of the synthesis of $Pd_2(dmb)_2(CN)_4$ will be published elsewhere. For the related compounds $Ni_2(dmb)_2(CN)_4$ and $Pd_2(dmb)_2I_4$ see also refs 16c and 16d, respectively. (b) Che, C.-M.; Yam, V. W.-W.; Wong, W.-T.; Lai, T.-F. *Inorg. Chem.* **1989**, *28*, 2908. (c) Gladfelter, W. L.; Gray, H. B. *J. Am. Chem. Soc.* **1980**, *102*, 5909. (d) Che, C.-M.; Herbstein, F. H.; Schaefer, W. P.; Marsh, R. E.; Gray, H. B. *Inorg. Chem.* **1984**, *23*, 2572.

(17) (a) Larson, A. C. *Acta Crystallogr.* **1967**, *23*, 664. (b) Gabe, E. J.; Lee, F. L.; LePage, Y. In *Crystallographic Computing: Data Collection, Structure Determination, Proteins and Databases*; Sheldrick, G. M., Kruger, C., Goddard, R., Eds.; Clarendon Press: Oxford, England, 1985; pp 167–174. (c) Cromer, D. T., Waber, J. T. In *International Tables for X-Ray Crystallography*; Ibers, J. A., Hamilton, W. C., Eds.; Kynoch Press: Birmingham, England, 1974; Vol. IV, Table 2.2B, pp 99–101 (present distributer: Kluwer Academic Publishers, Dordrecht, The Netherlands).

A Patterson map was interpreted in terms of $C2/m$, and the successful refinement confirms that choice. The data were corrected for a slight decay and for absorption; Lorentz and polarization factors were applied, and the two independent data sets were merged to give the final 2011 reflections. The R factor for merging the 1472 reflections with just two observations was 0.046.

The gold and phosphorus atom locations were obtained from the Patterson map, and the carbon and fluorine positions were found in a subsequent Fourier map. Full-matrix least-squares refinement with isotropic thermal parameters gave an R index of 0.2; hydrogen atoms were introduced at optimized positions based on difference maps calculated in their planes, anisotropic thermal parameters were assigned, and refinement of all the non-hydrogen atom parameters converged with an R index of 0.050 for the 1540 reflections with $F_o^2 > 3\sigma(F_o^2)$. The final difference map was noisy, with peaks of 2.31 and −2.72 e Å^{-3} at the gold atom position and excursions of 1.58 and −1.18 e Å^{-3} elsewhere. The dmpm ligand could have been disordered, and we checked for electron density in the alternate positions of the three carbon atoms; there is a peak where an alternate C1 would be, but nothing in the other two positions. The absorption correction for this crystal is large, and any error in measuring the crystal would have caused systematic errors in the data, leading to the problems we observed.

Calculations were done with programs of the CRYM Crystallographic Computing System and ORTEP. Scattering factors and corrections for anomalous scattering were taken from a standard reference.[17c] $R = \sum||F_o| - |F_c||/\sum F_o$, for only $F_o^2 > 0$, and goodness of fit = $[\sum w(F_o^2 - F_c^2)^2/(n-p)]^{1/2}$ where n is the number of data and p the number of parameters refined. The function minimized in least squares was $\sum w(F_o^2 - F_c^2)^2$, where $w = 1/\sigma^2(F_o^2)$. Variances of the individual reflections were assigned on the basis of counting statistics plus an additional term, $(0.014I)^2$. Variances of the merged reflections were determined by standard propagation of error plus another additional term, $(0.014\langle I\rangle)^2$. The absorption correction was done by Gaussian integration over an 8 × 8 × 8 grid. Transmission factors varied from 0.051 to 0.140. The secondary extinction parameter[17a] refined to 0.75 (6) × 10^{-6}.

Results and Discussion

Structure Descriptions. $Ag_2(dmpm)_2Br_2$ exhibits a $Ag_2(dmpm)_2^{2+}$ core structure with two silver atoms bridged by the dmpm ligands to give eight-membered $Ag_2P_4C_2$ rings, similar to the structure of $[Ag_2(dmpm)_2](PF_6)_2$ except that the molecule belongs to the C_i point group instead of C_{2h} (see Figure 1). The intramolecular $r(Ag_2)$ value (3.605 (2) Å) is much longer than the one for $[Ag_2(dmpm)_2](PF_6)_2$ ($r(Ag_2)$ = 3.041 (2) Å) and is caused by the presence of two Ag–Br coordination interactions on each silver atom that results in formation of a distorted tetrahedron around these atoms (Br–Ag–Br = 93.06 (4)°, P–Ag–P = 133.69 (9)°).[18] These AgBr interactions result in a polymeric $(Ag-(\mu\text{-dmpm})_2-Ag-(\mu\text{-Br})_2)_n$ structure in the solid state (Figure 2). The Ag–Ag···Ag angle (146.44 (3)°) differs from 180°; this deviation is due to the asymmetric $Ag-(\mu\text{-Br})_2-Ag$ unit (see structure I) where two distinct r(AgBr) values are measured

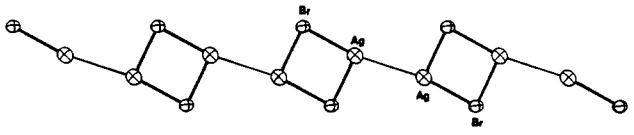

I

the $(-Ag-(\mu\text{-Br})_2-Ag-)_n$ polymeric chain (chain quasi-planar and infinite; dmpm ligands not shown)

(r(AgBr) = 2.7431 (13) and 2.9453 (13) Å). These r(AgBr) values compare well with those for the $Ag_3(dppm)_3Br_2^+$, cation for which two bromide atoms cap a cyclic Ag_3 core with six AgBr bonds ranging from 2.784 (4) to 2.942 (4) Å.[19] These r(AgBr) values indicate that the AgBr bonds possess significant ionic character.[20]

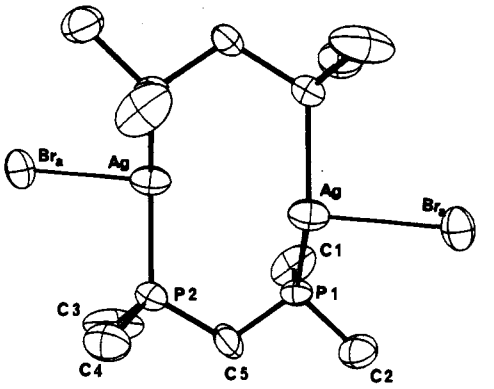

Figure 1. Molecular structure and atom labeling for $Ag_2(dmpm)_2Br_2$. The ORTEP drawing is shown with 50% probability ellipsoids.

Table II. Molecular Geometry for $Ag_2(dmpm)_2Br_2$

(a) Intramolecular Bond Lengths (Å) with Esd's in Parentheses

Ag–Br	2.9453 (14)	P1–C2	1.754 (10)
Ag–Br$_a$	2.7431 (13)	P1–C5	1.795 (9)
Ag–P1	2.4339 (25)	P2–C3	1.790 (10)
Ag–P2	2.429 (3)	P2–C4	1.756 (10)
P1–C1	1.806 (10)	P2–C5	1.871 (11)

(b) Valence Angles (deg) with Esd's in Parentheses

Br–Ag–Br$_a$	93.06 (4)	C1–P1–C2	100.4 (5)
Br–Ag–P1	101.09 (7)	C1–P1–C5	101.4 (5)
Br–Ag–P2	95.15 (7)	C2–P1–C5	102.8 (6)
Br$_a$–Ag–P1	104.38 (7)	Ag–P2–C3	114.3 (3)
Br$_a$–Ag–P2	116.73 (7)	Ag–P2–C4	114.7 (4)
P1–Ag–P2	134.69 (9)	Ag–P2–C5$_b$	122.6 (3)
Ag–Br–Ag$_a$	86.94 (4)	C3–P2–C4	101.6 (6)
Ag–P1–C1	115.5 (3)	C3–P2–C5	100.1 (5)
Ag–P1–C2	120.5 (4)	C4–P2–C5	100.4 (6)
Ag–P1–C5	113.6 (4)	P1–C5–P2	112.8 (5)

Table III. Distances and Angles Not Involving Hydrogen for $[Au_2(dmpm)_2](PF_6)_2$

Distances (Å)

Au–Au	3.045 (1)	P2–F1	1.46 (2)
Au–P1	2.289 (3)	P2–F2	1.44 (2)
P1–C1	1.83 (2)	P2–F3	1.40 (2)
P1–C2	1.835 (17)	P2–F4	1.37 (3)
P1–C3	1.76 (2)		

Angles (deg)

P1–Au–P1	178.3 (1)	F3–P2–F1	89.6 (12)
C1–P1–Au	111.9 (6)	F4–P2–F1	90.1 (16)
C2–P1–Au	115.5 (6)	F1–P2–F1	85.0 (10)
C3–P1–Au	113.7 (7)	F2–P2–F1	177.7 (11)
C2–P1–C1	96.5 (8)	F3–P2–F2	92.3 (13)
C3–P1–C1	113.9 (9)	F4–P2–F2	88.0 (16)
C3–P1–C2	104.1 (9)	F2–P2–F2	87.6 (11)
P1–C1–P1	116.6 (10)	F4–P2–F3	179.5 (17)
F2–P2–F1	93.7 (11)		

The large deviation of the P–Ag–P angle from that of a normal two-coordinate structure (180°) strongly suggests that the AgBr interactions are important. In the $Au_2(diphos)_2X_2$ complexes (diphos = dppm, dmpm, dmpe, cdpp ($(C_6H_5)_2P)_2C(CH_2)_2$); X = Cl, Br, I), the gold–halogen bonds are also long and presumably weak, and give rise to numerous types of structures.[21] In these cases, the P–Au–P angle also deviates slightly from 180° (ranging from 164 to 176°).[8a-i] On the other hand, the P–Ag–P angles in the $Ag_2(dppm)_2(NO_3)_2$ (138.3 (1)°),[7a] $[Ag_4(dppm)_4(NO_3)_2](PF_6)_2$ (152.0 (1)°),[7a] $[Ag_2(dppm)_2(NO_3)_2]\cdot CHCl_3$ (149.4 (1)°),[7b] and $Ag_2(dmpm)_2Br_2$ (133.69 (9)°) complexes are significantly smaller and are essentially intermediate values between 180 and 120° (ideal trigonal-planar structure) or between 180 and 113.5° (ideal tetrahedral structure). This difference in

(18) The halogen-bridging and chelating interactions are not unique in silver chemistry. See for example: Yamamoto, Y.; Aoki, K.; Yamazaki, H. *Inorg. Chim. Acta* **1982**, *68*, 75.

(19) Aly, A. A. M.; Neugebauer, D.; Orama, O.; Schubert, U.; Schmidbaur, H. *Angew. Chem., Int. Ed. Engl.* **1978**, *17*, 125.

(20) The ionic radii (r_{ion}) for Ag^+ and Br^- are 1.08 and 1.87 Å, respectively. The covalent radii (r_{cov}) for Ag and Br are 1.44 and 1.14 Å, respectively. See: Cotton, F. A.; Wilkinson, G.; Gauss, P. L. *Basic Inorganic Chemistry*, 2nd ed.; Wiley: Toronto, 1987; p 60.

(21) Puddephatt has recently surveyed the structural properties of the $Au_2(diphos)_2X_2$ complexes (X = halogen). See ref 8g.

Table IV. Structural Comparison for $[Au_2(dmpm)_2]Y_2$ Complexes

compd	$r(Au_2)$/Å	r(AuP)/Å	PAuP/deg	ref
$[Au_2(dmpm)_2](PF_6)_2$	3.045 (1)	2.289 (3)	178.3 (1)	this work
$[Au_2(dmpm)_2](ClO_4)_2$	3.028 (2)	2.313 (5)	178.0 (3)	8h
$[Au_2(dmpm)_2]Cl_2 \cdot 2H_2O$	3.010 (1)	2.300 (4)	176.61 (5)	8e
$[Au_2(dmpm)_2]Cl_2 \cdot 2H_2O$	3.014 (1)	2.303 (2)	176.80 (3)	8g
$[Au_2(dmpm)_2]Br_2 \cdot 2H_2O$	3.023 (1)	2.304 (2)	176.7 (1)	8h
$[Au_2(dmpm)_2]I_2 \cdot 2H_2O$	3.019 (1)	2.302 (3)	177.42 (7)	8b
$[Au_2(dmpm)_3](BF_4)_2$	3.040 (1), 3.050 (1)	2.344 (7)–2.384 (7)		8f

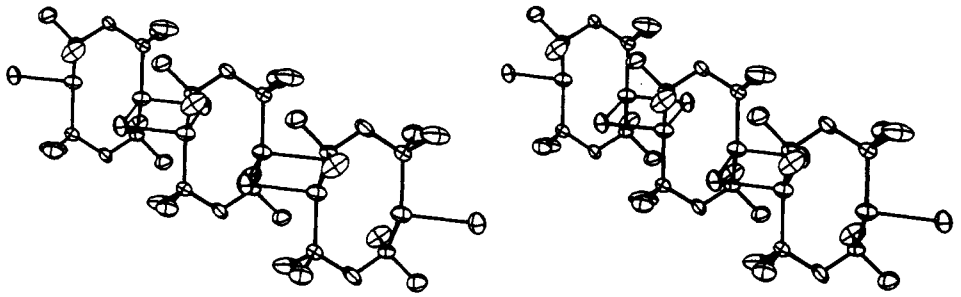

Figure 2. Stereoview of the crystal packing. The polymeric chain is infinite.

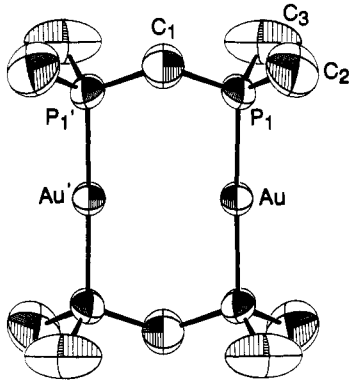

Figure 3. ORTEP drawing of the gold cation. Thermal ellipsoids are shown at the 50% probability level.

molecular distortions between Ag_2 and Au_2 must be due primarily to an electronic effect. The AgP (2.4339 (25), 2.429 (3) Å) and other bond distances and angles are all normal (Table II).

The intermolecular $r(Ag_2)$ value (3.916 (2) Å) is too great for any significant Ag–Ag interaction. On the other hand, the intramolecular Ag distance (3.605 (2) Å) is only slightly larger than twice the van der Waals radius (3.4 Å),[22] which suggests that very weak Ag interactions are present. The very weak intramolecular Au_2 interactions in $Au_2(dmb)_2(CN)_2$ are also confirmed by Raman spectroscopy (see text below). For $Ag_2(dmpm)_2Br_2$, a similar situation occurs.

The $[Au_2(dmpm)_2](PF_6)_2$ X-ray structure (Table III) exhibits a $Au_2P_4C_2$ ring adopting a chair conformation (Figure 3). $r(Au_2)$, 3.045 (1) Å, falls outside the typical range for Au–Au single bonds (ca. 2.757–2.780 Å)[22] but is well within twice the van der Waals radius (3.4 Å).[22] The $Au_2(dmpm)_2^{2+}$ core structure changes only slightly as a function the counteranion ($[Au_2(dmpm)_2]Y_2$; Y = ClO_4, PF_6, Cl, Br, I) where $r(Au_2)$, r(AuP), and the PAuP angles range from 3.010 (1) to 3.045 (1) Å, from 2.289 (3) to 2.313 (5) Å, and from 176.7 (1) to 178.3 (1)°, respectively (Table IV). The r(AuP) value for $[Au_2(dmpm)_2](PF_6)_2$ is the same as some Au–$P(C_6H_5)_3$ and Au–$P(C_2H_5)_3$ bond lengths,[23a-c] while other AuP bonds have been measured to be much shorter—2.22–2.24 Å.[23d,e] The phosphorus–carbon bond lengths are also normal, although that to C3 (the carbon atom with the largest thermal motion) is somewhat short (1.76 (2) Å vs 1.83 (2) Å for the other two). Bond angles are as expected, with P1–Au–P1′ equal to 178.3 (1)° and the angles at P1 ranging from 96.5 (8) (C1–P1–C2) to 115.5 (6)° (Au–P1–C2). The P1–C1–P1 angle is 116.6 (10)°. Interestingly, the $r(M_2)$ values in both $[M_2(dmpm)_2](PF_6)_2$ complexes (M = Ag, Au) are essentially identical (3.041 (2) Å, M = Ag;[7c] 3.0444 (17) Å, M = Au), which suggests that the relativistic effects in the 5s orbital of Ag compared to the 6s orbital of Au may not be important in these cases.[24]

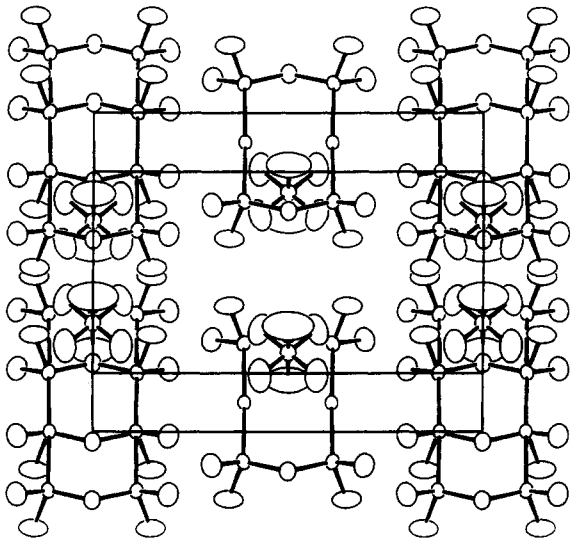

Figure 4. A unit cell and all its contents, plus the gold complexes that are partially inside and partially outside the cell. Thermal ellipsoids are shown at the 20% probability level.

The hexafluorophosphate group shows extreme apparent thermal motion or disorder, but the atom positions correspond to octahedral coordination with slightly short P–F bonds (1.418 (42) Å). The F–P–F angles deviate from 90 or 180° by an average of 2.1 (16)°.

In the cell, gold dimers are stacked along the b axis (Figure 4) with no close contacts between them (F···H contacts are about

(22) (a) Bondi, A. *J. Phys. Chem.* **1964**, *68*, 441. (b) Mingos, D. M. P. *Gold Bull.* **1984**, *17*, 5.

(23) (a) Bosman, W. P.; Bos, W.; Smits, J. M. M.; Beurskens, P. T.; Bou, J. J.; Steggerda, J. J. *Inorg. Chem.* **1986**, *25*, 2093–2096. (b) Hormann, A. L.; Shaw, C. F., III; Bennett, D. W.; Reiff, W. M. *Inorg. Chem.* **1986**, *25*, 2093–2096. (c) McNair, R. J.; Nilsson, P. V.; Pignolet, C. H. *Inorg. Chem.* **1985**, *24*, 1935–1939. (d) Casalnuovo, A. L.; Laska, T.; Nisson, P. V.; Olofson, J.; Pignolet, L. H. *Inorg. Chem.* **1985**, *24*, 233–235. (e) Price, S. J. B.; DiMartino, M. J.; Hill, D. T.; Kuroda, R.; Mazid, M. A.; Sadler, P. J. *Inorg. Chem.* **1985**, *24*, 3425–3434.

(24) Mason, Rodgers, et al.[8h] have argued that the relativistic effects were apparent from the comparison of $r(Au_2)$ and $r(Ag_2)$, between $[Au_2(dmpm)_2]Y_2$ (Y = ClO_4, Cl, Br) and $[Ag_2(dmpm)_2](PF_6)_2$, where $r(Au_2)$ ranges from 3.01 to 3.03 Å in comparison with $r(Ag_2)$ = 3.04 Å. The presence of the counteranion, Y^-, slightly affects $r(Au_2)$.[8h]

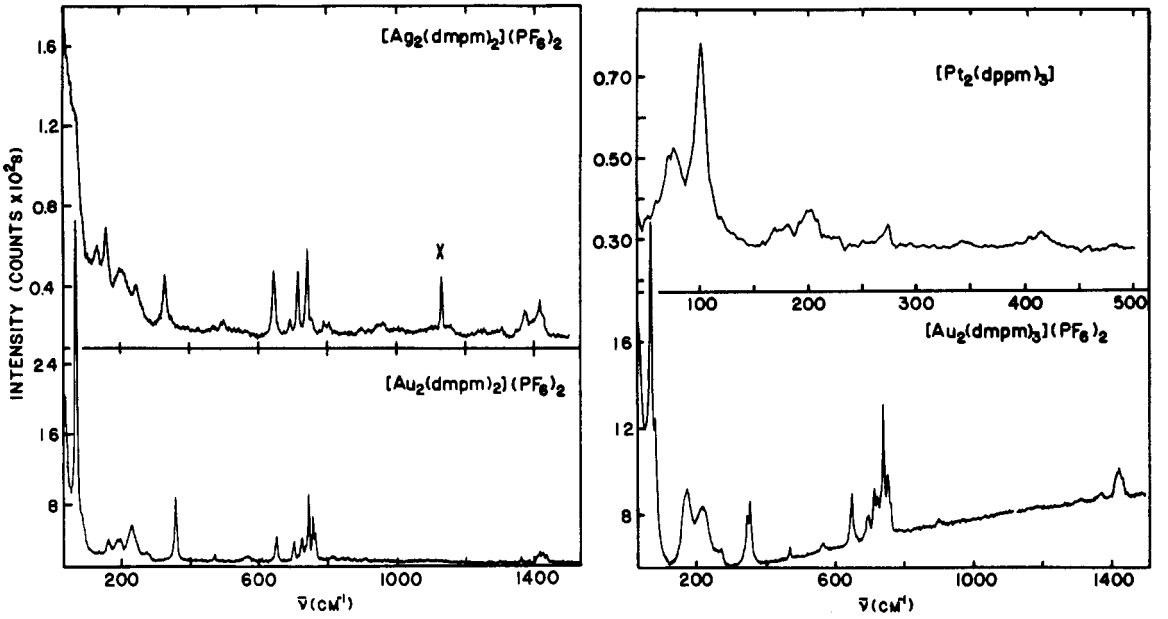

Figure 5. Raman spectra of microcrystalline $Pt_2(dppm)_3$, $[Au_2(dmpm)_3](PF_6)_2$, $[Au_2(dmpm)_2](PF_6)_2$, and $[Ag_2(dmpm)_2](PF_6)_2$. Experimental conditions: laser excitation 514.5 nm, laser power 5–10 mW at the sample, 300-μm slits, 2 s/point at every 1 cm^{-1}, 32× objective, the scan (except for $[Ag_2(dmpm)_2](PF_6)_2$, three scans), 298 K.

Table V. Vibrational Data for the Triply Bridged Diphosphine Binuclear Complexes[a]

$Pd_2(dppm)_3$		$Pt_2(dppm)_3$		$[Ag_2(dppm)_3](PF_6)_2$		$[Au_2(dmpm)_3](PF_6)_2$		
IR	R	IR	R	IR	R	IR	R	assgnt[b]
363				360	364	355		
340		350	349	350			345	ν(M–P)
325		338		334	325	326		
298		296						
285		268	273					δ(C–P–C)
250		226	249	259	240	273	269	
220		213						
198		196	200	215	211	222	220	δ(P–M–P)
165		169	175	144	190	210	174	
						100		
	120		102		77		68	ν(M–M)
	61		74		46		80	lattice mode?

[a] In the solid state, 298 K; cm^{-1}. [b] δ = deformation mode.

Table VI. Vibrational Data for the Doubly Bridged Diphosphine Binuclear Complexes[a]

$Ag_2(dmpm)_2Br_2$		$[Ag_2(dmpm)_2](PF_6)_2$		$[Au_2(dmpm)_2](PF_6)_2$		$[Au_2(dmpm)_2]Cl_2$		
IR[c]	R	IR	R	IR	R	IR	R	assgnt[b]
		347	351		355	348	362	ν(M–P)
320	325	323	327	339		334	352	
	272				271	275	271	δ(C–P–C)
245		250	246			258	248	
	230				228		232	
		213	203				216	
~184	~189				188	196	185	δ(P–M–P)
		154	160		162		172	
138	152		134				162	
	115			114		129		
					96 sh	104		
						81	91	ν(Au–Cl)
	75							ν(Ag–Br)?
				77				
	49		75		69		71	ν(M–M)
		88		64			62	lattice modes?
	24				38			

[a] In the solid state, 298 K; cm^{-1}. [b] δ = deformation mode. [c] The 30–100-cm^{-1} region has not been investigated.

2.8–3.0 Å). The closest approach to the gold atoms is from a fluorine atom (F3 at $x, y, 1 + z$), 3.42 Å; a hydrogen atom from C2 in a different cation is equally close. Neither of these contacts is in the direction of the gold–gold axis. This distance is long but compares with those for the $[Au_2(dmpm)_2]Y_2$ complexes (Y = ClO_4, Cl, Br, I),[8] where the gold···oxygen and gold···halide distances range from 3.32 (8) to 3.67 (8) Å.

Low-Frequency Vibrational Spectra. The 400–4000-cm^{-1} region is the diphosphine (and diisocyanide) ligand fingerprint, and very little changes are observed upon complexation with silver or gold atoms (see Figure 5 as an example); this region has not been investigated in this work. The lower frequency region is analyzed

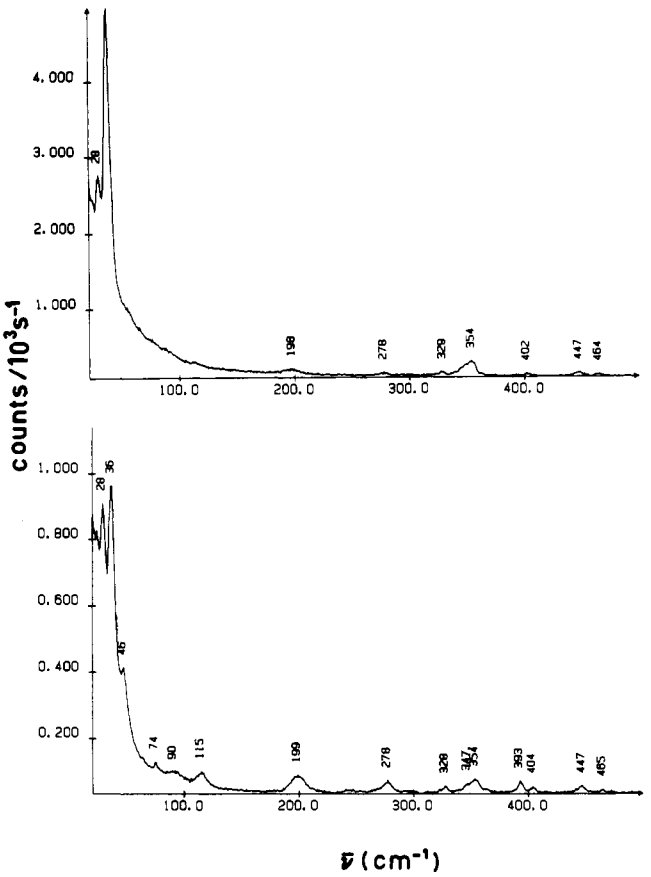

Figure 6. Raman spectra of a single crystal (0.5 × 0.5 × 1 mm) of $Au_2(dmb)(CN)_2$: (top) spectrum where the laser polarization is parallelly oriented with respect to the *z* crystal axis which is also along the Au_2 axis in the single crystal; (bottom) same experiment as above except the crystal was rotated by 90°. Experimental conditions are identical to those for Figure 4. The top spectrum is essentially identical to the powder spectrum in which weak features are difficult to observe. The bottom spectrum allows a better analysis of the Raman data.

using assignments made by different research groups for complexes of the type $M_2(dppm)_2X_2$[25] and $M_2(dppm)_3$[6a,9c] (M = Pd, Pt; X = Cl, Br, I) and other related compounds.[25b,c] The investigated diphosphine complexes are divided into two categories, M_2L_6 and M_2L_4, and their vibrational analyses are given in Tables V and VI, respectively. For comparison purposes, the $M_2(dppm)_3$ data are also included.

The vibrational mode of interest, $\nu(M_2)$, is identified directly from the comparison of the known Raman $Pt_2(dppm)_3$ spectrum[9c] with the isostructurally related $[Au_2(dmpm)_3](PF_6)_2$ spectrum, where $\nu(M_2)$ is the most intense scattering (Figure 5). Moving from $[Au_2(dmpm)_3](PF_6)_2$ to $[Au_2(dmpm)_2](PF_6)_2$, no major spectral change occurs; $\nu(Au_2)$ (68 cm^{-1}) still dominates the spectrum. The replacement of gold by silver in the $[M_2(dmpm)_2](PF_6)_2$ complexes induces only small frequency shifts for a few peaks. In addition, the $\nu(Ag_2)$ band does not appear as a strong peak but rather as a shoulder (~76 cm^{-1}). A relatively weak $\nu(Ag_2)$ band is also observed in the $[Ag_2(dppm)_3](PF_6)_2$ spectra. The Raman spectrum of $[Au_2(dmpm)_2]Cl_2$ is essentially the same as that of $[Au_2(dmpm)_2](PF_6)_2$ with some added complexity presumably reflecting the lower symmetry. Interestingly, a new feature of medium intensity located at 91 cm^{-1} (81 cm^{-1} in the IR spectrum) appears in the $[Au_2(dmpm)_2]Cl_2$ spectra and could be assigned to $\nu(AuCl)$ ($r(AuCl)$ = ca. 3.46 Å).[8c]

For the two weakly interacting dimers, $Au_2(dmb)(CN)_2$ and $Ag_2(dmpm)_2Br_2$ (Figures 6 and 7), we assign $\nu(Au_2)$ = 36 and $\nu(Ag_2)$ = 48 cm^{-1}.[26] To support this assignment, the solid-state $Pd_2(dmb)_2(CN)_4$ Raman spectrum has also been recorded. For $Pd_2(dmb)_2(CN)_4$, $r(Pd_2)$ is expected to be ~4.4 Å with no Pd···Pd interactions.[27,28] Indeed, the $Pd_2(dmb)_2(CN)_4$ spectrum exhibits practically the same vibrational features (at slightly different frequencies)[29] as those for $Au_2(dmb)(CN)_2$, with the obvious

Table VII. Spectroscopic and Structural Data for Very Weakly Interacting Metallic Dimers

	$\nu(M_2)$/ cm^{-1}	$F(M_2)$/mdyn $Å^{-1}$ [a]	$r(M_2)$/ Å	$2r_{vdW}$/ Å [b]
$Ag_2(dmpm)_2Br_2$	48[c]	*d*	3.60[c]	3.40
$Au_2(dmpm)_2(CN)_2$	36[c]	0.075	3.54[e]	3.40
$Hg_2(^1\Sigma_g^+)$	18.5[f]	0.020	3.63[f]	3.00
$Hg_2(^1\Sigma_u^+)$	19.7[f]	0.023	3.61[f]	3.00
$Cd_2(^1\Sigma_g^+)$	58[g]	0.111		3.20
$Ca_2(^1\Sigma_g^+)$	64.92[h]	0.050	4.28[h]	
$Cs_2(^1\Sigma_g^+)$	42.02[h]	0.069	4.47[h]	
$Mg_2(^1\Sigma_g^+)$	51.12[h]	0.019	3.89[h]	3.40

[a] $F(M_2) = \mu(2\pi c\nu(M_2))^2$; μ = reduced mass. [b] $2r_{vdW}$ = sum of the van der Waals radii; from ref 22. [c] From this work. [d] Estimated to be ~0.03 mdyn $Å^{-1}$ (see text). [e] From ref 8j. [f] From ref 11. [g] Matrix experiments. Nakamoto, K. *Infrared and Raman Spectra of Inorganic and Coordination Compounds*, 4th ed.; Wiley: New York, 1987. [h] Huber, K. P.; Herzberg, G. *Molecular Spectra and Molecular Structure Constants of Diatomic Molecules*; Van Nostrand: New York, 1979.

Table VIII. Structural and Spectroscopic Data for the Au_2 Compounds

	$\nu(Au_2)$/ cm^{-1}	$\nu(Au_2)$/mdyn $Å^{-1}$ [a]	$r(Au_2)$/ Å
$Au_2(dmb)(CN)_2$	36[b]	0.075	3.536[c]
$Au_2(tmb)Cl_2$	50[d]	0.14[d]	3.301[d]
$Au_2(ylide)_2$	64[e]	0.24	2.977[f]
$[Au_2(dmpm)_3](PF_6)_2$	68[b]	0.27	3.045
$[Au_2(dmpm)_2](PF_6)_2$	69[b]	0.28	3.044[b]
$[Au_2(dmpm)_2]Cl_2$	71[b]	0.29	3.010[g]
$Au_2(ylide)_2Cl_2$	162[e]	1.98[k]	2.597[h]
$Au_2^-(^2\Sigma_u^+)$	149[i]	1.29	2.582[i]
$Au_2(^3\Sigma_u^+)$	142[j]	1.18	2.568[j]
$Au_2(^1\Sigma_u^+)$	180	1.88	2.520[j]
$Au_2(^1\Sigma_u^+)$	191[j]	2.11	2.472[j]

[a] Unless stated otherwise, $F(M_2) = \mu(2\pi c\nu(M_2))^2$; μ = reduced mass. [b] This work. [c] From ref 8j. [d] From ref 10. [e] From ref 31. [f] Basil, J. D.; Murray, H. H.; Fackler, J. P., Jr.; Tocher, J.; Mazany, A. M.; Trzcinska-Bancroft, B.; Knachel, H.; Dudis, D.; Delord, T. J.; Marler, D. O. *J. Am. Chem. Soc.* **1985**, *107*, 6908. Ylide = $(CH_2)_2P(C_6H_5)_2$. [g] From ref 8e. [h] Schmidbaur, M.; Mandl, J. R.; Frank, A.; Muttner, G. *Chem. Ber.* **1976**, *109*, 466. Ylide = $(CH_2)_2P(C_2H_5)_2^-$. See also footnote *f* and the references therein in which $r(Au_2)$ (2.61 Å) for $Au_2(ylide)_2Br_2$ ylide = $(CH_2)_2P(C_6H_5)_2^-$) is reported. [i] Bauschlicher, C. S., Jr.; Langhoff, S. R.; Partridge, H. *J. Chem. Phys.* **1989**, *91*, 2412 and the reference therein. [j] Huber, K. P.; Herzberg, G. *Molecular Spectra and Molecular Structure Constants of Diatomic Molecules*; Van Nostrand: New York, 1979. [k] Calculated from the equations for X-M-M-X systems[33] and neglecting the off-diagonal force constant because only the symmetric ν(M-X) is known (ν(Au-Cl) = 293 cm^{-1}).[31]

(25) (a) Alves, O. L.; Virtorge, M.-C.; Sourisseau, C. *Nouv. J. Chim.* **1983**, *7*, 231. (b) Duddell, D. A.; Goggin, P. L.; Goodfellow, R. J.; Norton, M. G.; Smith, J. G. *J. Chem. Soc. A* **1970**, 545. (c) Rojhantalab, H.; Nibler, J. W.; Wilkins, C. J. *Spectrochim. Acta* **1976**, *32A*, 519.

(26) (a) These values are at the borderline of the lattice vibration (ν_L) zone for complexes of the type $M_2(dppm)_2X_2$ (M = Pd, Pt; X = Cl, Br) where $0 < \nu_L < 40$ cm^{-1} (see ref 25). (b) $Au_2(dmb)(CN)_2$ exists in its syn form in solutions, with no Au···Au interactions (Perreault, D.; Harvey, P. D. Unpublished results). Hence solution Raman experiments can neither confirm nor disprove the $\nu(Au_2)$ assignments. Similarly, $Au_2(dmpm)_2Br_2$ exhibits ligand exchange at room temperature as in $[Ag_2(dppm)_3]^{2+}$ [13] and $[Ag_2(dmpm)_3]^{2+}$.[26c] (c) Dean, P. A. W.; Vittal, J. J.; Srivastava, R. S. *Can. J. Chem.* **1987**, *65*, 2628.

(27) (a) The $r(M_2)$ values for $Ni_2(dmb)_2(CN)_4$,[16c] $Pd_2(dmb)_2I_4$,[16d] and $Pd_2(dmb)_2Cl_4$[27b] are 4.33, 4.58, and 4.40 Å, respectively. (b) Perreault, D.; Drouin, M.; Michel, A.; Harvey, P. D. Submitted for publication.

(28) The Pd···Pd separations (4.3–4.6 Å) are too long to expect any Pd_2 interaction. The van der Waals radius is 1.6 Å.[22]

Table IX. Structural and Spectroscopic Data for the Ag_2 Compounds

	$\nu(Ag_2)$/cm^{-1}	$F(Ag_2)$/mdyn Å^{-1} [a]	$r(Ag_2)$/Å	Woodruff's $r(Ag_2)$/Å [b]
$Ag_2(dmpm)_2Br_2$	48[c]		3.601[c]	
$[Ag_2(dppm)_3](PF_6)_2$	76[c]	0.18	3.10 ± 0.01[d]	3.18
$[Ag_2(dmpm)_2](PF_6)_2$	76[c]	0.18	3.041[e]	3.18
$Ag_2^-(^2\Sigma_u^+)$	118[f]	0.44	2.814[f]	3.05
Ag_3	120.5[g]			
$Ag_2(^1\Sigma_g^+)$	192.4[g]	1.18	2.471[f]	2.74

[a] $F(M_2) = \mu(2\pi c\nu(M_2))^2$; μ = reduced mass. [b] Calculated using eq 1. [c] This work. [d] Average values for various $Ag_2(dppm)_2^{2+}$ complexes taken from refs 7a,b. It is assumed that $r(Ag_2)$ is only slightly affected by the counteranions and the number of diphosphine bridging ligands (see Table IV for example). [e] From ref 7c. [f] Bauschlicher, C. S., Jr.; Langhoff, S. R.; Partridge, H. *J. Chem. Phys.* **1989**, *91*, 2412 and reference therein. [g] Schulze, W.; Becker, H. V.; Minkwitz, R.; Manzel, K. *Chem. Phys. Lett.* **1978**, *55*, 59. For Ag_3, the authors have suggested that the molecule is linear ($F(Ag_2)$ = 0.916 mdyn Å^{-1}).

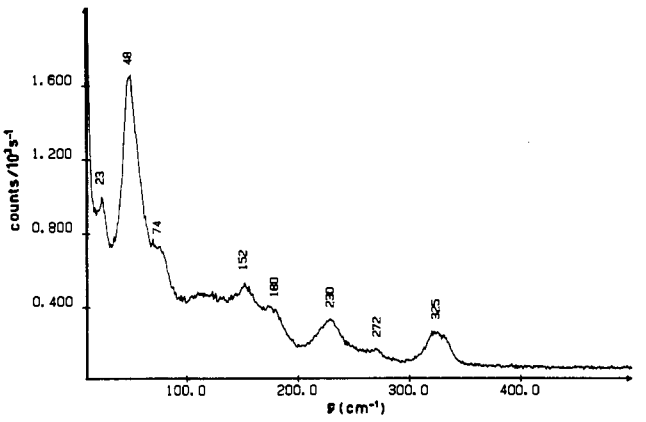

Figure 7. Raman spectrum of solid $Ag_2(dmpm)_2Br_2$. Experimental conditions are idential to those for Figure 4.

exception that no strong band appears between 25 and 45 cm^{-1}. For $Au_2(dmb)(CN)_2$, the $\nu(Au_2)$ assignment (36 cm^{-1}) is further supported as the associated $F(Au_2)$, 0.075 mdyn Å^{-1}, follows a linear relationship for ln F vs r (see following section).

For $Ag_2(dmpm)_2Br_2$, the lower 48 cm^{-1} value is consistent with the longer $r(Ag_2)$ with respect to $[Ag_2(dmpm)_2](PF_6)_2$ and is also consistent with the even lower 36 cm^{-1} datum measured for the heavier binuclear system $Au_2(dmb)(CN)_2$. Interestingly, the presence of very weak M_2 interactions is not unique to $Ag_2(dmpm)_2Br_2$ and $Au_2(dmb)(CN)_2$. Indeed, Table VII lists the $\nu(M_2)$, $F(M_2)$, and $r(M_2)$ data for M_2 compounds where $r(M_2)$ > 3.5 Å. These literature data compare well with those for $Ag_2(dmpm)_2Br_2$ and $Au_2(dmb)(CN)_2$ and support the assignments.

Force Constants and Metal–Metal Separations. Literature results provide $\nu(Au_2)$ and $r(Au_2)$ data for some other Au_2 compounds and are listed in Table VIII. In most cases, $F(Au_2)$ can be readily extracted from the diatomic approximation and as expected $F(Au_2)$ decreases with $r(Au_2)$. The estimated $r(Au_2)$ values from Woodruff's rules (see eq 2) compare surprisingly poorly with the experimental data (see details in the supplementary material). On the other hand, a plot of $r(Au_2)$ versus ln $F(Au_2)$ (Figure 8) gives a reasonable linear relationship going from 2.4 to 3.6 Å:

$$r(Au_2) = -0.290 \ln F(Au_2) + 2.68 \quad (3)$$

where the correlation coefficient (σ) is 0.97 (11 data points). This equation is essentially a reparametrized H–L equation applied soley to Au_2 systems. The graph can be separated into two zones;

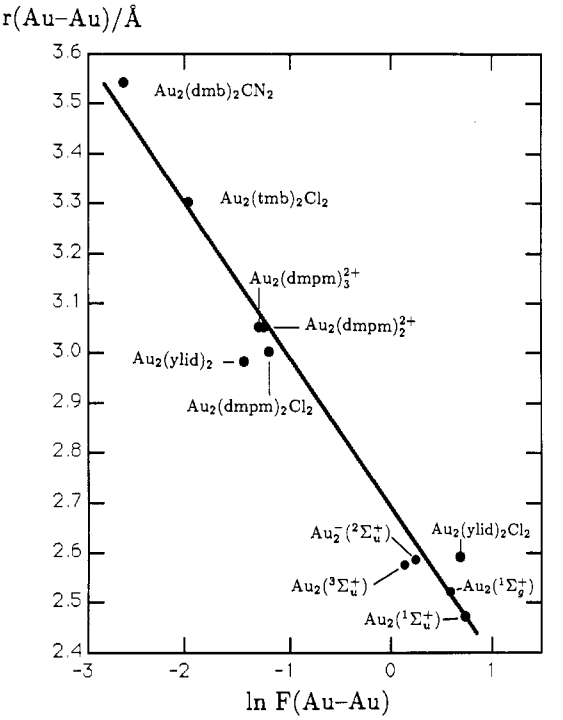

Figure 8. Graph of ln $F(Au_2)$ vs $r(Au_2)$.

the singly bonded Au_2 ($r(Au_2)$ < 2.6 Å) and the formally nonbonded Au_2 ($r(Au_2)$ > 2.9 Å). It is not possible to verify whether this relationship applies to Au_2 compounds with bond order larger than 1 since, to our knowledge, no such complexes have been synthesized.

The comparison between the calculated $r(Au_2)$ from eq 3 and the experimental results is reasonably good (within 2%). The largest differences are found for the two ylide complexes (3 and 5%). In these cases, it is possible that the $F(Au_2)$ values approximated using the diatomic model could be wrongly estimated due to the "rigid" ylide ligand.

The obvious application for empirical relationships is the estimation of $r(Au_2)$ directly from Raman data (when $F(Au_2)$ can be obtained confidently, or vice versa). For instance, Fackler, Clark, et al.[30] have recently argued that the $\nu(Au_2)$ assignment for $Au_2(S_2CN(C_4H_9))_2$ ($\nu(Au_2)$ = 185 cm^{-1}; $F(Au_2)$ = 1.95 mdyn Å^{-1};[31] $r(Au_2)$ = 2.76 Å[32]) was too great to be reasonable. They suggested that $\nu(Au_2)$ would range between 60 and 105 cm^{-1} for this compound. Equation 3 estimates that the calculated $r(Au_2)$ value would be 2.49 Å for $F(Au_2)$ = 1.95 mdyn Å^{-1}. On the other hand, using $r(Au_2)$ = 2.76 Å as the starting point, eq 3 gives

(29) (a) The vibrational spectra are not interpreted in detail (IR 114 m, 132 w, 167 w, 188 w, 219 w, 349 w, 369 m, 397 m, 405 m cm^{-1}; Raman 49 m, 67 m, 104 w, 129 w, 184 w, 281 w, 314 w, 346 w, 370 w, 398 w cm^{-1}; m = medium, w = weak). The 50–400-cm^{-1} region includes ν(M–L), skeleton deformation and torsion modes. Complete vibrational analysis for compounds of the type MX_4^{n-} (M = Au(III), Pt(II), Pd(II); X = Cl, Br, I)[29b] and of the type $M(CN)_2^-$ (M = Ag, Au)[29c] are available. (b) Hendra, P. J. *J. Chem. Soc. A* **1967**, 1298. (c) Adams, D. M.; Fletcher, P. A. *Spectrochim. Acta* **1988**, *44A*, 437.

(30) Clark, R. J. H.; Tocker, J. H.; Fackler, J. P., Jr.; Neira, R.; Murray, H. H.; Knackel, H. *J. Organomet. Chem.* **1986**, *303*, 437.
(31) Farrell, F. J.; Spiro, T. G. *Inorg. Chem.* **1971**, *10*, 1606.
(32) (a) Åkerstrom, S. *Ark. Kemi* **1959**, *14*, 387. (b) Hesse, R. In *Advances in the Chemistry of Coordination Compounds*; Kirschner, S., Ed.; Macmillan: New York, 1961; p 314.

$F(Au_2)$ and $\nu(Au_2)$ values of 0.76 mdyn Å^{-1} and 114 cm^{-1}, respectively, not 185 cm^{-1}. For $Au_2(S_2CN(C_4H_9)_2)_2$, the closest Raman feature is found at 138 cm^{-1} and was attributed to a Au-S-C deformation on the basis of polarization data. These observations are consistent with those of Fackler, Clark, et al.,[30] and it appears that the $Au_2(S_2CNR_2)_2$ spectra need to be reinvestigated.

The $F(Ag_2)$ value for $Ag_2(dmpm)_2Br_2$ cannot be accurately obtained using conventional equations (diatomic model, valence force field expressions for linear X-M-M-X units[33]). The diatomic model suggests that $F(Ag_2)$ would be 0.073 mdyn Å^{-1}, while the valence force field equations cannot be solved.[34] In the former case, the presence of quasi-linearly bonded bromides (r(AgBr) = 2.74 Å) has been wrongly ignored. Nevertheless, the main conclusion from these simple calculations is that $F(Ag_2)$ is indeed small. Vibrational and structural literature data for Ag_2 compounds are scarce. Only four data points have been used (Table IX) in order to approximate a relationship similar to eq 3:

$$r(Ag_2) = -0.30 \ln F(Ag_2) + 2.5 \quad (4)$$

Using $r(Ag_2)$ = 3.60 Å, a value of 0.03 mdyn Å^{-1} is calculated for $F(Ag_2)$. This value compares favorably with those listed in Table VII and is consistent with the fact that for similar $r(M_2)$ values (3.60 Å for $Ag_2(dmpm)_2Br_2$ and 3.54 Å for $Au_2(dmb)(CN)_2$), $F(Ag_2)$ should be smaller than $F(Au_2)$.[35]

Acknowledgment. This research was supported by the NSERC and FCAR. D.P. thanks the Université de Sherbrooke for an institutional graduate fellowship. W.P.S. and V.M.M. thank the NSF for Grant CHE-8219039 to purchase the diffractometer and the Exxon Educational Foundation for financial support. P.D.H. acknowledges Professor I. S. Butler (McGill University) for providing access to the Raman instruments and Mr. Y. Huang (McGill University) and Dr. Fran Adar (ISA) for technical assistance in the measurements of some of the Raman spectra.

Registry No. $Ag_2(dmpm)_2Br_2$, 137945-44-9; $[Au_2(dmpm)_2](PF_6)_2$, 137945-45-0; $Pd_2(dppm)_3$, 37266-95-8; $Pt_2(dppm)_3$, 37266-96-9; $[Ag_2(dppm)_3](PF_6)_2$, 137964-62-6; $[Ag_2(dmpm)_2](PF_6)_2$, 81343-14-8; $Pd_2(dmb)_2(CN)_4$, 137945-46-1; $Au_2(dmb)(CN)_2$, 124719-87-5; $Au_2(dmpm)_2Cl_2$, 137945-47-2.

Supplementary Material Available: Tables of atomic coordinates, bond distances, bond angles, anisotropic thermal parameters, and hydrogen atom positions for $Ag_2(dmpm)_2Br_2$ and $[Au_2(dmpm)_2](PF_6)_2$ and a table showing a comparison between the Woodruff and reparametrized Herschbach-Laurie rules for Au_2 compounds (5 pages); listings of observed and calculated structure factors (18 pages). Ordering information is given on any current masthead page.

(33) Herzberg, G. *Molecular Spectra and Molecular Structure*; Van Nostrand: New York, 1945; Vol. II, p 180.

(34) Assuming that the assignment for the Raman-active ν(AgBr) at 75 cm^{-1} is correct (for the quasi-linear Br-Ag-Ag-Br moieties shown in structure I, r(AgBr) = 2.74 Å), the valence force field calculations for an X-M-M-X system (ignoring the presence of perpendicularly bonded phosphine and weakly bonded bromine (r(AgBr) = 2.9 Å) yield imaginary solutions.

(35) (a) For the isostructural $M_2(dppm)_3$ complexes (M = Pd, Pt) where $r(M_2) \sim 3.0$ Å,[35b] the $F(M_2)$ values are 0.45 (M = Pd) and 0.60 mdyn Å^{-1} (M = Pt).[6a] (b) Manojlovic-Muir, L. J.; Muir, K. W.; Grossel, M. C.; Brown, M. P.; Nelson, C. P.; Yavari, A.; Kallas, E.; Moulding, R. P.; Seddon, K. R. *J. Chem. Soc., Dalton Trans.* **1986**, 1955. (c) Kirss, R. V.; Eisenberg, R. *Inorg. Chem.* **1989**, *28*, 3372.

Contribution from the Department of Chemistry, Kent State University, Kent, Ohio 44242

Electron Transfer. 111. Disproportionation of Carboxylato-Bound Chromium(IV). Catalysis by Manganese(II)[1]

M. C. Ghosh,* E. Gelerinter, and E. S. Gould*

Received May 22, 1991

Tetrapositive chromium, Cr(IV), a state stabilized in aqueous solution through ligation by anions of branched α-hydroxy acids, undergoes decay by a combination of disproportionation ($2Cr^{IV} \rightarrow Cr^{III} + Cr^{V}$) and ligand oxidation. In solutions having pH 2.5-4.0, buffered by 2-ethyl-2-hydroxybutanoic acid (HLig) and its anion (Lig^-), disproportionation is very nearly quantitative and is found to be catalyzed markedly by Mn(II). Both the Cr(V) and Cr(III) products are bis chelates. In the absence of Mn(II), the disproportionation is second order in Cr(IV), and observed variation of rates with $[H^+]$ and $[Lig^-]$ points to a predominant reaction path entailing reactions of two units of the deprotonated complex, $Cr^{IV}(OH)$, which species is also an important contributor to the Mn(II)-catalyzed reaction. For the latter, a nonlinear rate dependence on $[Mn^{II}]$ indicates the formation of a Cr(IV)-Mn(II) adduct (K = 52). Bridged precursor complexes are suggested for both the uncatalyzed (Cr^{IV}-O-Cr^{IV}) and catalyzed (Cr^{IV}-OH-Mn^{II}) reactions, and it is proposed that the catalyzed path involves a rate-determining conversion of Mn(II) to Mn(III), a state having a $1e^-$ reduction potential near the gap between those for Cr(IV,III) and Cr(V,IV). In addition to this potential constraint, it is desirable that ligand substitutions about both states of the catalyst be more rapid than those about Cr(IV). Among the various $1e^-$ redox couples derived from other d- and f-block metal centers, only Ce(IV,III) appears to conform to these requirements, but action in this case is complicated by preferential oxidation of the ligand by Ce(IV).

Both atypical oxidation states of chromium, Cr(V)[2] and Cr(IV),[3] may be stabilized in solution through chelation by anions of branched α-hydroxy acids such as 2-ethyl-2-hydroxybutanoic acid (I). However, the two states are not equally persistent.

$$(C_2H_5)_2C(OH)COOH$$
I

Aqueous solutions of Cr(V), in the presence of an excess of the ligating anion, remain virtually unchanged in the dark at room temperature for up to 24 h, whereas Cr(IV) solutions, given comparable conditions, suffer perceptible loss within a few minutes. The latter state undergoes both disproportionation (eq 1) and

$$2Cr(IV) \rightarrow Cr(III) + Cr(V) \quad (1)$$

$$2Cr(IV) + R_2C(OH)COO^- \rightarrow 2Cr(III) + R_2C{=}O + CO_2 + H^+ \quad (2)$$

reduction by the parent ligand (eq 2) with the relative importance of these two modes of attrition dependent both on the acidity of the medium and on the nature and concentration of added transition-metal ions.

(1) Sponsorship of this work by the National Science Foundation (Grant 9019840) is gratefully acknowledged.

(2) See, for example: (a) Krumpolc, M.; DeBoer, B. B.; Roček, J. *J. Am. Chem. Soc.* **1978**, *100*, 145. (b) Krumpolc, M.; Roček, J. *Ibid.* **1979**, *101*, 3206. (c) Gould, E. S. *Acc. Chem. Res.* **1986**, *19*, 66.

(3) (a) Ghosh, M. C.; Gould, E. S. *Inorg. Chem.* **1990**, *29*, 4258. (b) *Ibid.* **1991**, *30*, 491.

0020-1669/92/1331-0702$03.00/0